

An Improved PSO-Based Maximum Power Point Tracking Algorithm for Distributed Photovoltaic System Under Partial Shading

Yanxuan Zheng , Yan Li , Yangpeng Guo, Ye Tian , Fangyi Wei , Yi Tian 

Electrical Engineering School of Beijing Jiaotong University, China

Corresponding author: Yan Li, liyan@bjtu.edu.cn

Abstract

Module-level power electronics with distributed characteristics makes it possible to significantly improve the output power of traditional centralized photovoltaic(PV) systems in the case of series or parallel mismatches. However, for distributed PV systems, when partial shading occurs in a single PV module, there will still be multiple local extreme points on its Power-voltage(P-V) characteristic curve, forming a multi-peak feature, which makes traditional maximum power point tracking(MPPT) methods ineffective and unable to find the true maximum power point of the module. Therefore, this paper takes advantage of module-level power electronics, and designs the four-switch Buck-Boost converter as the module-level power optimizer for distributed PV systems. At the same time, the paper focusing on the module multi-peak seeking optimization problem in distributed PV power systems, proposes a module-level multi-peak MPPT optimization algorithm based on the improved particle swarm optimization(PSO), which utilizes an improved particle swarm optimization algorithm based on the traditional perturbation observation method in order to perform a global search for multi-peaks. Compared to the traditional PSO algorithm, the proposed algorithm operates on the principle of prioritizing particles that are closer to the global best power value, which filters the initial positions and search areas of the particles. This approach reduces the number of iterations needed in the tracking process, decreases power oscillations during transient tracking of the maximum power point, and improves the tracking accuracy of the traditional PSO algorithm.

1 Introduction

Photovoltaic (PV) power generation is an effective solution for alleviating the fossil energy crisis and environmental pollution problems, which has a broad development prospect. In PV systems, the output characteristics of PV arrays and PV strings are nonlinear and are influenced by irradiance and ambient temperature. Under fixed irradiance and temperature conditions, there exists a unique maximum power point (MPP) for PV arrays and PV strings. Therefore, in order to improve the efficiency of PV power generation systems, Maximum Power Point Tracking (MPPT) technology has received widespread attention. Compared with the centralized MPPT of traditional PV systems using inverters, distributed MPPT can significantly maximize the power output and reduce the power mismatch losses under most of mismatch conditions in PV arrays and strings, such as differences in irradiance between modules, temperature variations, aging differences, and varying orientations and tilt angles of different modules[1],[2].

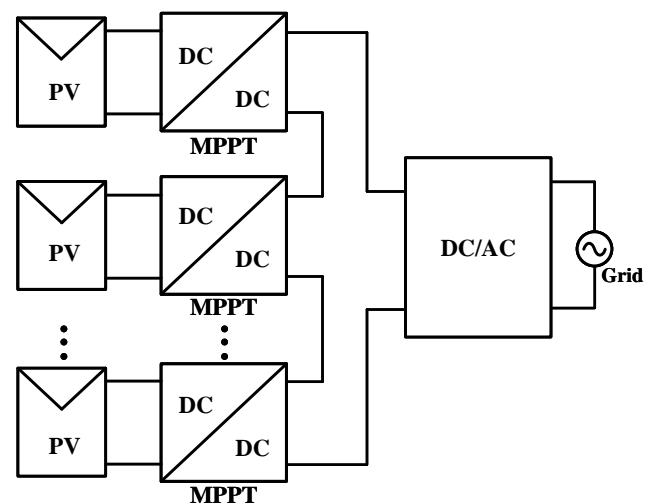


Fig. 1: Distribute power electronics architecture of power optimizers.

Distributed MPPT includes module-level MPPT and submodule-level MPPT. By employing power electronic converters as control modules, it enables independent MPPT control for individual modules or even single substrings within a module. This effectively resolves mismatch issues in the series

and parallel connections of traditional PV arrays or PV strings. The DC/DC power optimizer for module-level MPPT is currently the mainstream distributed power electronic architecture for PV system. As shown in Fig. 1, the output of each PV panel is connected to a DC-DC converter (power optimizer) to achieve single-panel MPPT control, and then the outputs of these power optimizers are connected in series for connecting to a grid-tied inverter[2]. Additionally, outputs of optimizers also are connected in parallel before connecting to the subsequent inverter at some applications[3]. And in cases of series and parallel mismatches in PV arrays, power optimizers utilizing module-level MPPT technology can recover 3% to 16% or more of the power loss[4],[5].

However, the actual output power level of a distributed PV system is still constrained by the current operating conditions of the modules. Factors such as buildings, fallen leaves, and bird droppings can cause some modules to operate under partial shading conditions, leading to multiple peaks on the P-V characteristic curve of these modules[1], as shown in Fig. 2. Traditional MPPT methods, such as the Perturb and Observe (P&O) method and the Incremental Conductance method can accurately track the maximum power in the P-V curve with a single peak. However, under partial shading conditions, where the P-V curves have multiple peaks, these traditional methods tend to get trapped in local maximum peaks and fail to identify the true maximum power point[6].

To address the challenge of tracking the MPP on a P-V curve with multiple peaks under partial shading conditions, multi-peak MPPT methods of scanning P-V curve has been developed. Traditional global scanning methods examine the entire P-V curve at fixed intervals to find the MPP, but this approach results in significant energy loss due to prolonged searches in the non-maximum power region. Literature[7],[8] have improved the traditional global scanning process, and literature[8] made reasonable assumptions about local peak power changes on both sides of the global power point to improve the tracking speed, which are not suitable for all working conditions.

Compared to global scanning methods, MPPT optimization based on meta-heuristic algorithms[9] such as Particle Swarm Optimization (PSO), Grey Wolf Optimization, Artificial Ant Colony Algorithm, with stochastic behavior characteristics, improve

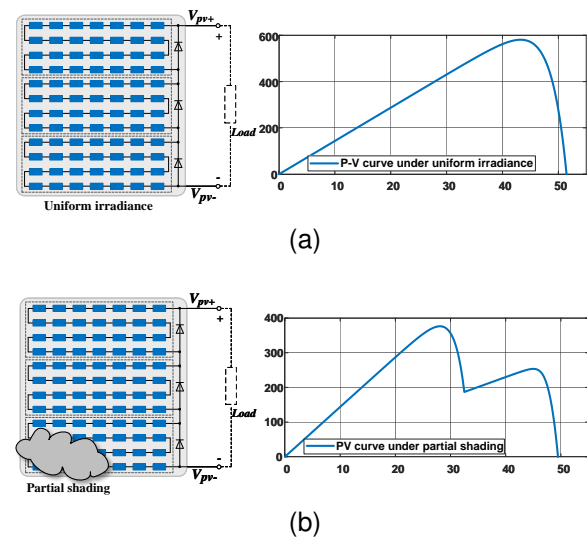


Fig. 2: PV curve of single module. (a) Single-peak curve of the module under uniform irradiance. (b) Multi-peak curve of the module under partial shading.

the ability to jump out of local peak region to a certain extent, and have advantages of finding the MPP more quickly. Among these, the PSO MPPT algorithm has become a popular research topic. However, traditional PSO algorithms suffering from complicated parameter adjustments makes it challenging to maintain tracking accuracy under multi-peak conditions, and they are prone to significant transient power oscillations during the tracking process. Literature[10] simplified the parameter settings during the tracking process, reducing both the number of searches and transient power oscillations. Nonetheless, the initialization and search process in [10] is overly complex, making it difficult to implement in practical optimizers.

Therefore, based on the distributed control capability of module-level power optimizers, this paper proposes a module-level multi-peak MPPT optimization algorithm with improved PSO. This algorithm builds upon traditional Perturb and Observe methods, employing improved PSO algorithm for global search across multiple peaks. The proposed approach simplifies initialization and search stages by prioritizing particles close to the global maximum power value for initial selection, optimizing their initial positions and search regions, and reducing the iteration count during tracking process. It also mitigates power oscillations during transient tracking of the MPP. The main sections of this paper are structured as follows: Section 2 introduces the distributed MPPT technology of power optimizers, Section 3 details the proposed multi-peak MPPT optimization algorithm, Section 4 provides valida-

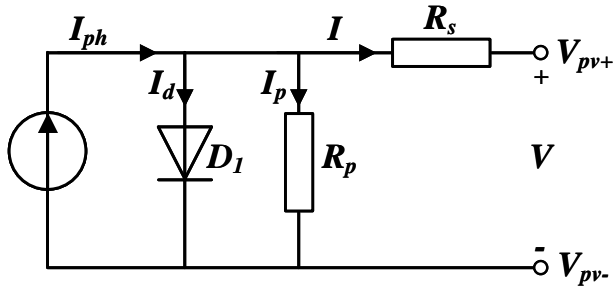


Fig. 3: The equivalent circuit diagram of the PV cell.

tion using MATLAB and compares it with the traditional PSO algorithm, and Section 5 presents the conclusions.

2 Distributed MPPT Technology of Power Optimizers

PV systems are highly susceptible to partial shading and other environmental factors. The practical operation of PV systems often involves mismatch conditions, resulting in decreased output power from mismatched PV modules. Therefore, the Distributed Maximum Power Point Tracking method connects each PV module to an individual DC/DC converter, allowing for independent MPPT on each module, which recovers some of the power losses caused by partial shading. Module-level MPPT has been widely implemented in power optimizers, with various power ratings available on the market. However, partial shading increases the number of local MPPs, making module-level MPPT implementation more challenging, which is the focus of this paper.

2.1 Multi-peak Characteristics of Photovoltaic Modules

The equivalent circuit diagram of the PV cell is shown in Fig. 3. According to Kirchhoff's law, relationship between the output current I of the PV cell and the voltage U across the cell can be expressed by Eq. (1),

$$I = I_{ph} - \frac{U + I \cdot R_s}{R_{sh}} - I_d \quad (1)$$

where I_{ph} is the photogenerated current, I_d is the dark current of the diode, R_s is the equivalent series resistance and R_{sh} is the equivalent parallel resistance. To improve power generation efficiency, photovoltaic cells are usually connected in series to form PV modules, which serve as the smallest power generation units within the PV system.

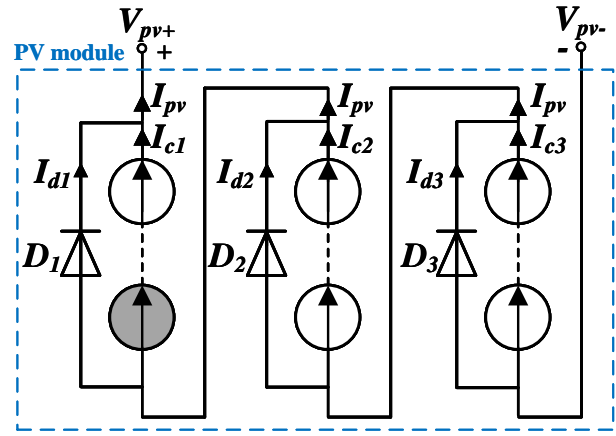


Fig. 4: Internal schematic diagram of a PV module with three bypass diodes.

$$\begin{cases} I_{ci} = I_{pv}, & I_{pv} \leq I_{ph(min)} \quad (i = 1, 2, 3) \\ I_{ci} = I_{ph(min)}, & I_{pv} > I_{ph(min)} \quad (i = 1, 2, 3) \end{cases} \quad (2)$$

$$I_{di} = I_{pv} - I_{ci} \quad (i = 1, 2, 3) \quad (3)$$

According to Eq. (1), when the output current I of all cells in the module is less than I_{ph} , the photovoltaic module generates power. However, if the photogenerated current I_{ph} of some cells in the module decreases due to partial shading and falls below the output current of other cells, those cells become loads, consuming energy and gradually forming hot spots. To mitigate this, bypass diodes are typically connected in parallel with a certain number of photovoltaic cells within the module. Typically, a module contains three bypass diodes, as shown in Fig. 4. I_{pv} is the module's output current, and I_{ci} is the sub-string cell current, with their relationship given in Eq. (2). $I_{ph(min)}$ is the minimum photogenerated current in the sub-string after shading. Thus, when partial shading occurs in the module, the bypass diodes provide an alternative current paths for the sub-strings which has reduced current, alleviating the hot spot issue. The on-state current of the bypass diode is shown in Eq. (3)

Therefore, partial shading reduces the photogenerated current of a substring within the module, which can be approximated as the short-circuit current. This results in steps in the I-V curve and multi-peak characteristics in the P-V curve of the module. The changes in the multi-peak characteristics of a PV module under different shading conditions is illustrated in Fig. 5, where the value of the short-circuit current of the module varies in proportion to

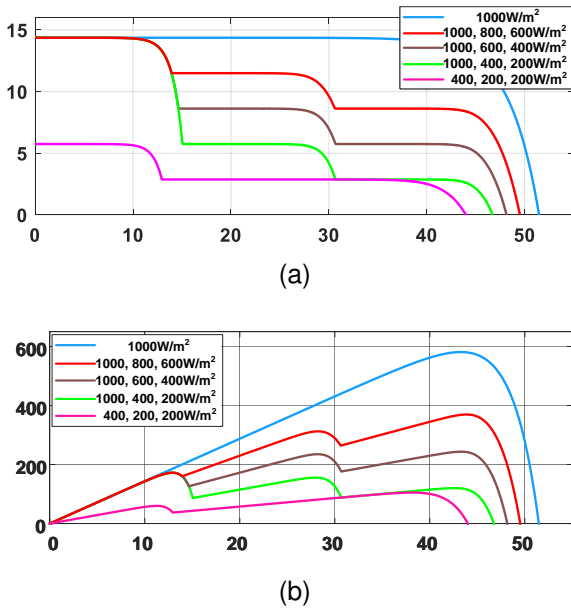


Fig. 5: Multi-peak characteristics curves of a single PV module under different shading conditions. (a) I-V characteristic curves. (b) P-V characteristic curves.

the irradiance, and the maximum number of multi-peaks appears to be the same as the number of bypass diodes of the module. In this paper, it is assumed that a PV module contains three bypass diodes, and the P-V curve of this PV module will have at most three peaks.

2.2 Module-level MPPT Control of Power Optimizers

Currently, series-type power optimizer architectures for distributed PV systems have been deployed in practical applications. Various power optimizer circuit topologies are available[11], including Buck converters, Boost converters, and Four-Switch Buck-Boost (FSBB) converters. The FSBB has distinct advantages due to its step-up and down capability, maintaining the same polarity between input and output. This feature significantly extends the MPPT voltage regulation range in series power optimizer systems, making the FSBB converter particularly beneficial for optimizing the performance of distributed PV systems. Consequently, this paper selects the FSBB converter as the power optimizer to perform module-level MPPT. The specific architecture is illustrated in Fig. 6, where the outputs of each power optimizer are connected in series to form a high-voltage DC bus. This bus is subsequently linked to the grid through an inverter or directly connected to other types of loads. Each photovoltaic module can perform MPPT indepen-

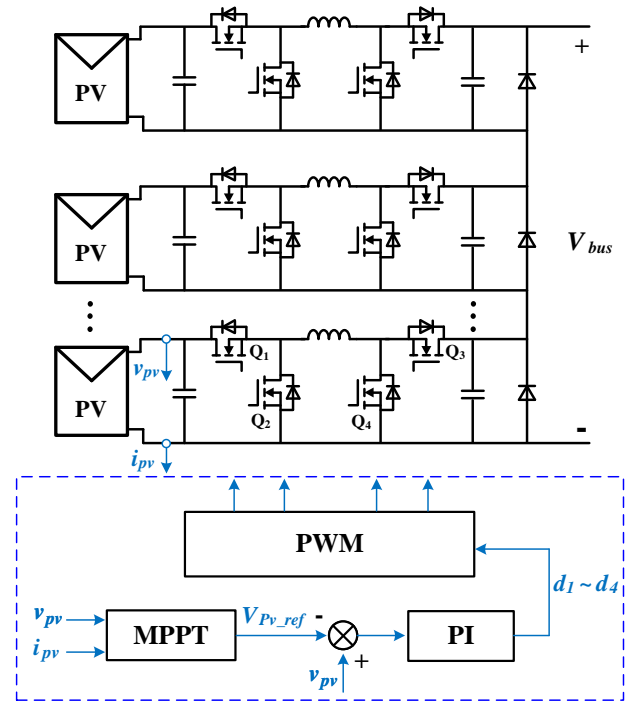


Fig. 6: Distributed photovoltaic system architecture with power optimizers using Four-Switch Buck-Boost (FSBB) converters.

dently through a power optimizer. For example, the MPPT control block diagram for one single power optimizer in the system is shown in Fig. 6.

3 Proposed MPPT Algorithm

The traditional PSO algorithm suffers from significant transient power oscillations and low tracking accuracy, which lead to substantial losses during the tracking process and ultimately reduce tracking efficiency. The factors affecting the reliability of the particle swarm algorithm can be summarized from the following aspects. Firstly, it's the particle initialization process, inappropriate initialization will lead to poor tracking effect. The second is the complex adjustment of numerous parameters, inappropriate adjustments may increase the number of iterations and prolong power oscillations. Thirdly, the iterative updating process exhibits an immediate nature that determines the generation of power fluctuations, which is also the essential drawback of the particle swarm algorithm and the focus of this paper.

The algorithm proposed in this paper based on the P&O approach adopts an improved PSO algorithm for global search to locate the maximum peak area. During the particle initialization process, the improved PSO algorithm prioritizes particles close to the global optimal power value, which based on

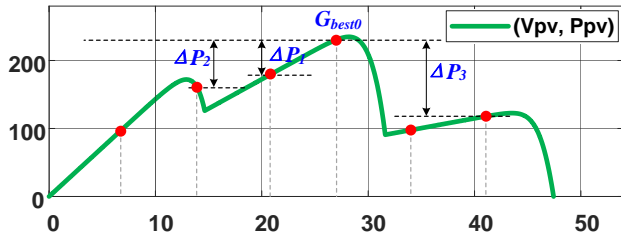


Fig. 7: The proposed improved PSO algorithm initialization process diagram.

a uniform distribution. In this paper, the voltage values on the P-V curve are used as the positions of the particles, and the power values are used as the fitness values of the particles. As illustrated in Fig. 7, using six particles as an example, the particle with the highest power in the initial stage is selected as the initial global best value, G_{best0} . The power differences between the remaining particles and G_{best0} are compared, and half of the particles that are far away from the global best initial value are eliminated, i.e., three particles with the largest ΔP_i are eliminated. The remaining three superior particles including G_{best0} proceed to the global search phase because $\Delta P_1 < \Delta P_2 < \Delta P_3$ with the ΔP_3 less than the other ΔP_i , thereby narrowing the search area.

$$x_i = r_1 P_{i,best} + (1 - r_1) G_{best} \quad (\text{for } i = 1, 2, 3) \quad (4)$$

$$\begin{cases} P_{i,best} = x_i, & f(x_i) > f(P_{i,best}) \\ P_{i,best} = P_{i,best}, & f(x_i) \leq f(P_{i,best}) \end{cases} \quad (5)$$

$$\begin{cases} G_{best} = P_{i,best}, & f(P_{i,best}) > f(G_{best}) \\ G_{best} = G_{best}, & f(P_{i,best}) \leq f(G_{best}) \end{cases} \quad (6)$$

In this paper, the parameters are simplified during the optimization iteration process. The principles of particle swarm optimization and the parameter simplification settings were based on the method described in [10]. The specific iterative process is detailed in Eq. (4) to Eq. (6). x_i is the position of the i th particle, r_1 is a random number between 0 and 1, $P_{i,best}$ is the personal best position found by the i th particle during the iterations, G_{best} is the global best position found by the particles in each iteration, $f(P_{i,best})$ is the power value corresponding to the individual particle's best position $P_{i,best}$ and $f(G_{best})$ is the power value corresponding to the global best

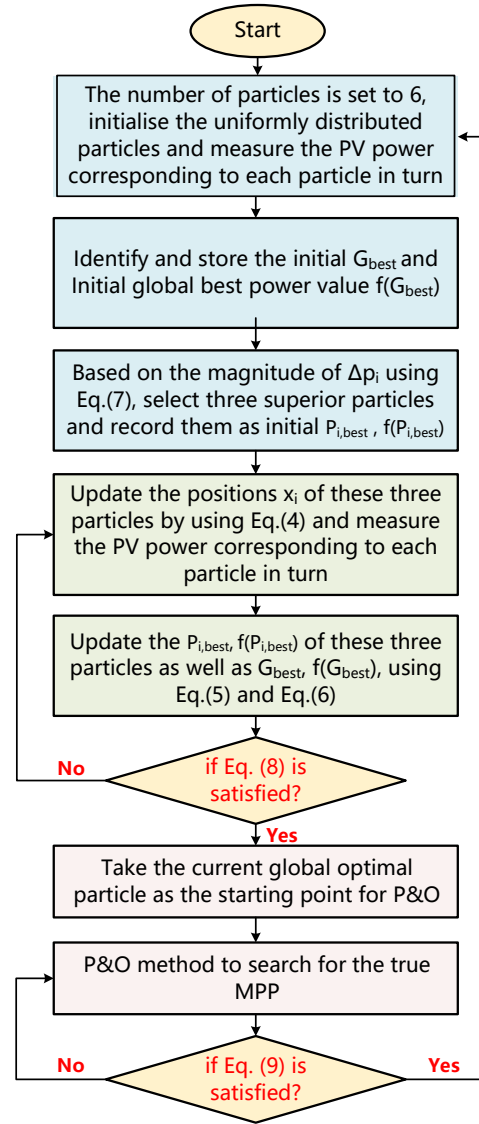


Fig. 8: The flowchart of the proposed improved PSO multi-peak MPPT algorithm.

position G_{best} . Each particle updates its current position according to G_{best} and $P_{i,best}$, and keeps comparing and updating G_{best} and $P_{i,best}$ during each iteration, so that after k iterations, all particles can converge towards the global best position.

$$\Delta P = |f(G_{best}) - f(P_{i,best})|, \quad P_{i,best} \neq G_{best} \quad (7)$$

$$\frac{|\max(\Delta P) - \min(\Delta P)|}{\min(\Delta P)} < 0.1 \quad (8)$$

$$\frac{|P_k - P_{k-1}|}{P_{k-1}} \geq 0.1 \quad (9)$$

When the ΔP shown in Eq. (7) of the three particles with respect to the current global best particle

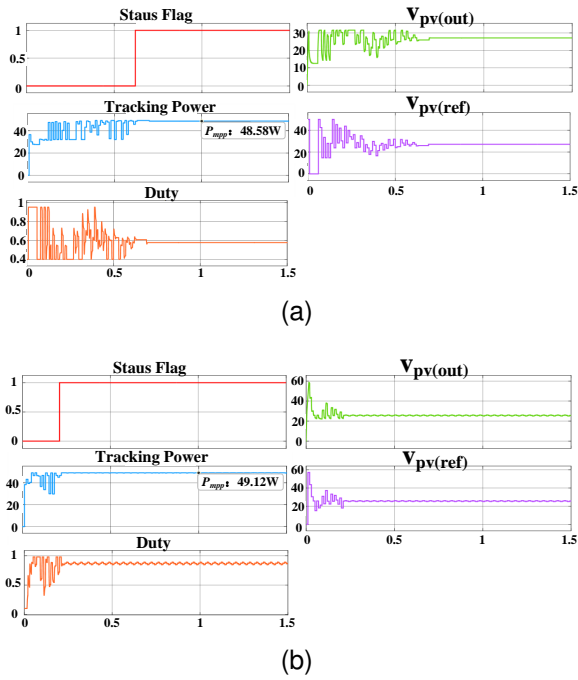


Fig. 9: Comparison of simulation results between conventional PSO MPPT and improved PSO MPPT under partial shading. (a) Conventional PSO MPPT. (b) Improved PSO MPPT.

satisfies Eq. (8), the algorithm finds the vicinity of the maximum power point and enters the local search mode. Taking the current global optimal particle as the starting point, the P&O method is used to accurately track the true maximum power point. Additionally, when there is a sudden change in shading conditions, the algorithm is reinitialized according to the conditions set in Eq. (9). The overall algorithm flowchart is shown in Fig. 8.

4 Simulation and Experimentation

4.1 Simulation

The MPPT optimization algorithm proposed in this paper is validated in MATLAB, which using a four-switch Buck-Boost optimizer circuit in the simulation, with an inductance of 9μH and a load set to 10Ω and the switching frequency is set to 100 kHz. The parameters of the PV module are presented in Tab. 1. At an irradiance of 1000 W/m², the maximum power is 101.3W. When partial shading occurs, i.e., at irradiance levels of 400 W/m² and 1000 W/m², double-peak cases have appeared, But the two peaks are close and difficult to distinguish. The actual voltage at the maximum power point is 25.74V, with a maximum power of 49.12W. While there is a local peak at a voltage of 53.85V, with a corresponding power of 44.42W. The im-

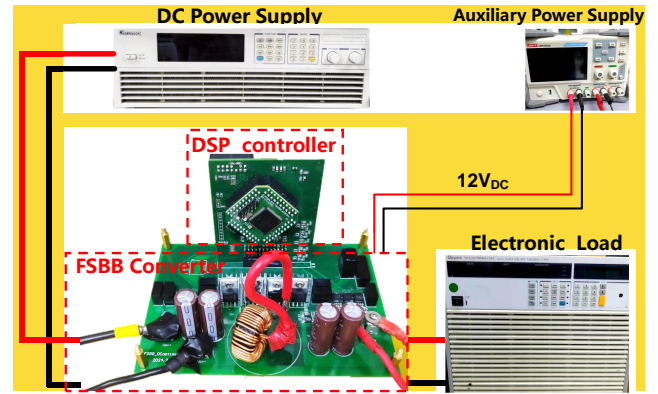


Fig. 10: The Power optimizer experimental platform of Four-Switch Buck-Boost (FSBB) converter.

Tab. 1: Simulation parameters of a PV module.

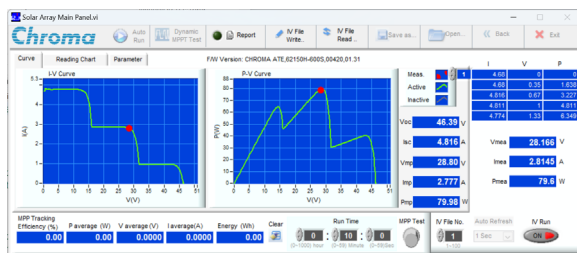
Parameter names	Parameter values
V_{oc}	70V
I_{sc}	2.22A
V_{mpp}	49.88V
I_{mpp}	2.00A
P_{mpp}	101.31W

proved PSO MPPT simulation results and the comparison of conventional PSO MPPT are depicted in Fig. 9. From the comparison results, it can be seen that the multi-peak MPPT optimization algorithm based on improved PSO proposed in this paper reduces the power oscillations during transient tracking of the MPP, and also improves the accuracy compared to the traditional PSO.

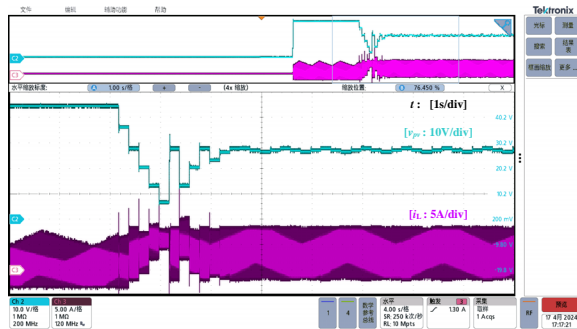
4.2 Experimentation

The FSBB optimizer platform is built to validate the proposed module-level multi-peak MPPT optimization algorithm based on the improved particle swarm optimization, as illustrated in Fig. 10. This experimental platform including the Chroma 62150H-600S photovoltaic simulator simulating the characteristics of actual photovoltaic modules, the DSP (Digital Signal Processor) TMS320F2800412 board serving as the control module for the FSBB converter board, the auxiliary power supply for chips within DSP board and FSBB converter, and an electronic load used as a resistive load.

The experiment simulates the MPPT tracking of one PV module under complex triple-peak conditions, with the maximum peak situates in the middle. Considering factors such as actual sampling delays, the time interval between two successive MPPT operations was set to 200ms in the experiment, which



(a)



(b)

Fig. 11: Experimental Results of improved multi-peak MPPT tracking with the global peak in middle.
(a) Tracking results shown in the PV simulator.
(b) Tracking process of the PV module output voltage V_{pv} .

is different from the ideal state of the simulation. The parameters of the PV module and the experimental results are presented in Fig. 11a. The tracking process of the PV module output voltage V_{pv} is shown in Fig. 11b. In this case, the theoretical maximum power was 79.98W, and the actual output power was 79.6W, and the improved multi-peak algorithm identified the global peak point within 2.6 seconds. In other cases involving single or double peaks, the proposed algorithm can also track the maximum power point effectively.

5 Conclusion

Partial shading occurring on PV modules invalidates the traditional module-level single-peak MPPT algorithm, resulting in the output power loss of distributed PV systems. This paper proposes a module-level multi-peak MPPT optimization algorithm based on the improved PSO method. The improved PSO algorithm operates on a global scale, reducing the number of iterations in the tracking process by refining the initial positions and search areas of the particles. Near the maximum peak, the P&O method is employed for precise searching. The proposed multi-peak MPPT algorithm combines the global search advantages of the PSO al-

gorithm with the local precision search capabilities of the P&O method. By prioritizing particles that are close to the global optimal power value, the algorithm mitigates power oscillation during the transient tracking process of the maximum power point and enhances the tracking accuracy compared to the traditional PSO algorithm.

6 References

- [1] J. D. Bastidas-Rodriguez, E. Franco, G. Petrone, C. A. Ramos-Paja, and G. Spagnuolo, "Maximum power point tracking architectures for photovoltaic systems in mismatching conditions: A review," *IET Power Electronics*, vol. 7, no. 6, pp. 1396–1413, 2014. DOI: <https://doi.org/10.1049/iet-pel.2013.0406>.
- [2] M. Kasper, D. Bortis, and J. W. Kolar, "Classification and comparative evaluation of pv panel-integrated dc-dc converter concepts," *IEEE Transactions on Power Electronics*, vol. 29, no. 5, pp. 2511–2526, 2014. DOI: 10.1109/TPEL.2013.2273399.
- [3] Y. Zheng, Y. Li, S. Sheng, B. Scandrett, and B. Lehman, "Distributed control for modular plug-and-play subpanel photovoltaic converter system," in *2017 IEEE Applied Power Electronics Conference and Exposition (APEC)*, 2017, pp. 1267–1271. DOI: 10.1109/APEC.2017.7930858.
- [4] S. M. MacAlpine, R. W. Erickson, and M. J. Brandemuehl, "Characterization of power optimizer potential to increase energy capture in photovoltaic systems operating under nonuniform conditions," *IEEE Transactions on Power Electronics*, vol. 28, no. 6, pp. 2936–2945, 2013. DOI: 10.1109/TPEL.2012.2226476.
- [5] A. J. Hanson, C. A. Deline, S. M. MacAlpine, J. T. Stauth, and C. R. Sullivan, "Partial-shading assessment of photovoltaic installations via module-level monitoring," *IEEE Journal of Photovoltaics*, vol. 4, no. 6, pp. 1618–1624, 2014. DOI: 10.1109/JPHOTOV.2014.2351623.
- [6] H. Oufettoul, S. Motahhir, G. Aniba, and I. Ait Abdelmoula, "Comprehensive analysis of mppt control approaches under partial shading condition," in *2022 11th International Conference on Renewable Energy Research and*

- Application (ICRERA)*, 2022, pp. 352–359. DOI: 10.1109/ICRERA55966.2022.9935687.
- [7] H. Patel and V. Agarwal, “Maximum power point tracking scheme for pv systems operating under partially shaded conditions,” *IEEE Transactions on Industrial Electronics*, vol. 55, no. 4, pp. 1689–1698, 2008. DOI: 10.1109/TIE.2008.917118.
- [8] K. S. Tey and S. Mekhilef, “Modified incremental conductance algorithm for photovoltaic system under partial shading conditions and load variation,” *IEEE Transactions on Industrial Electronics*, vol. 61, no. 10, pp. 5384–5392, 2014. DOI: 10.1109/TIE.2014.2304921.
- [9] S. Ahmed, S. Mekhilef, M. Mubin, K. S. Tey, and M. Kermadi, “An adaptive perturb and observe algorithm with enhanced skipping feature for fast global maximum power point tracking under partial shading conditions,” *IEEE Transactions on Power Electronics*, vol. 38, no. 9, pp. 11 601–11 613, 2023. DOI: 10.1109/TPEL.2023.3285243.
- [10] J. S. Koh, R. H. G. Tan, W. H. Lim, and N. M. L. Tan, “A modified particle swarm optimization for efficient maximum power point tracking under partial shading condition,” *IEEE Transactions on Sustainable Energy*, vol. 14, no. 3, pp. 1822–1834, 2023. DOI: 10.1109/TSTE.2023.3250710.
- [11] F. Wang, R. Gou, T. Zhu, Y. Yang, and F. Zhuo, “Comparison of dmppt pv system with different topologies,” in *2016 China International Conference on Electricity Distribution (CICED)*, 2016, pp. 1–5. DOI: 10.1109/CICED.2016.7576359.